Design of linear and nonlinear controller for DC-DC boost converter with right-half plane zero

T. Anitha* and S. Arulselvi

Department of Electronics and Instrumentation Engineering,
Annamalai University,
Annamalainagar, Tamilnadu, 608002, India
Email: rgm_anitha@rediffmail.com
Email: arulselvi_2k3@yahoo.co.in
*Corresponding author

Abstract: A major problem arises in the controller design when the transfer function of control-to-output voltage has right-half plane (RHP) zero. The effect of RHP zero predominates in the transfer functions of boost and buck-boost converters leading to a tedious controller design. Hence in this paper, the design of linear and nonlinear controllers for a DC-DC boost converter is discussed. Since the design of the linear controller (PI) strongly depends on the small signal transfer function of the converters, it leads to poor voltage regulation for wide variation in operating point. To overcome the above said difficulties and to achieve large signal stability, robustness, good dynamic response and simple implementation, an additional inner loop employing sliding mode control (SMC) with boundary layer is proposed in current mode control (CMC) scheme. Extensive simulation studies are carried out for DC-DC boost converter with RHP zero to verify the merits of SMC over PI controller using MATLAB/Simulink software.

Keywords: DC-DC converter; boost converter; RHP zero; sliding mode controller; PI controller.

Reference to this paper should be made as follows: Anitha, T. and Arulselvi, S. (2022) 'Design of linear and nonlinear controller for DC-DC boost converter with right-half plane zero', *Int. J. Power Electronics*, Vol. 15, No. 1, pp.116–130.

Biographical notes: T. Anitha received her BE, ME and PhD in Electronics and Instrumentation Engineering from Annamalai University in 1998, 2005 and 2016, respectively. She is currently working as an Associate Professor in the Department of Electronics and Instrumentation Engineering, Annamalai University, Tamilnadu. Her research interest includes intelligent control of power converters and drives.

S. Arulselvi received her BE in Instrumentation Engineering from GCT, Coimbatore. She received her ME in Instrument and Control from Anna University. Subsequently, she is awarded with Doctorate of Philosophy at Anna University, Chennai. At present, she is serving as a Professor in the Department of Electronics and Instrumentation Engineering, Annamalai University, Tamilnadu. She has been engaged in research work for the past 20 years in the area of power electronics and renewable energy systems.

1 Introduction

The DC-DC converters are widely used in industrial applications such as DC motor drives, computer systems, aerospace systems and communication equipments. The DC-DC converters can be viewed as dc transformer that deliver, DC voltage or current at a different level than the input source. DC-DC converters, classified as nonlinear systems are need to be averaged and linearised to obtain a linear time-invariant model and the design of high performance control for them is a challenging issue. The two general approaches to design feedback controllers for DC-DC converters are voltage mode control (VMC) and current mode control (CMC). The CMC is preferred over VMC, since it provides faster transient response, instantaneous overload protection and removes one pole from the control-to-output transfer function. Also, CMC provides input voltage feed-forward control. However, the controller design based on the above control methods becomes difficult, when a zero lies in the right-half plane (RHP) of the complex s plane. In the literature, it is reported that the control-to-output transfer function of boost, buck-boost, flyback and cuk converters exhibit RHP zero (Alvarez-Ramirez et al., 2001; Viswanathan et al., 2002). The presence of RHP zero tends to destabilise wide bandwidth feedback loops, because during a transient, the output initially changes in the wrong direction producing inverse response (IR) or non- minimum phase characteristic. It is also difficult to obtain an adequate phase margin since an additional phase lag of 90° is added, which alters the open loop phase angle of boost and buck-boost converters from –180° to –270°, thus limiting the value of controller gain. Hence, designers are forced to restrict the closed-loop bandwidth based on the worst-case RHP zero location to 1/30th of the switching frequency. As a result the system has a sluggish small signal and a poor large signal response. The effect of RHP zero predominates in the transfer functions of boost and buck-boost converters leading to a tedious controller design.

Hence in this work, the design of linear and nonlinear controllers for a DC-DC boost converter is discussed. To improve the dynamic response and to reduce the effect of RHP zero, conventional linear PI controller design using open-loop Ziegler-Nichols (Z-N) tuning method is discussed. The above mentioned controller is realised in VMC. Since the design of the linear controller strongly depends on the small signal transfer function of the converters, it leads to poor voltage regulation for wide variation in operating point. In addition, the controller designed under VMC provides satisfactory response for load changes but delays the response to supply voltage fluctuation. VMC also restricts the closed-loop bandwidth and the maximum achievable controller gain.

To overcome the above said difficulties and to achieve large signal stability, robustness, good dynamic response and simple implementation, an additional inner loop employing sliding mode control (SMC) with boundary layer is proposed in CMC scheme. The conventional PI controller is then designed for the outer loop (Arulselvi, 2007). The control laws are presented in detail using Flippov's method and Lynapov method for SMC. Extensive simulation studies are carried out for DC-DC boost converter with RHP zero to verify the merits of SMC over PI using MATLAB/Simulink software.

Recently many literatures have reported about the effects of RHP zero present in DC-DC converters and controllers' design to reduce its effect on the system response. Few of them have addressed the elimination of RHP zero in DC-DC converters.

By using a smaller value of inductor, low switching frequency and operating the converter in the discontinuous-conduction mode (DCM), the RHP zero can be eliminated.

But these techniques increase the ripple and peak currents of the converter components, thereby increasing the output filter requirements.

The design procedure of optimal and robust controller forCuk converter with RHP zero has been reported by many authors. This method is applicable only for single operating point with small parameter variations. Nonlinear proportional and integral (PI) controller based on the Z-N method was proposed for the regulation of the output voltage both in boost and buck-boost power converters with boost inductor value set at 20 mH. The effect of RHP zero on the system dynamics has not been brought out clearly. The experimental verification of the above algorithm will also be difficult.

Alvarez-Ramirez et al. (2001) discussed the design of PI controller based on gain parameterisation to provide insight into the inherent limitation induced by the RHP zero on the stability of boost converter. The analysis has been carried out with high inductor value of 43.5 mH, to reduce the ripple content in the load current. The design procedures are complex and the study of the effect of RHP zero on the transient response has not been reported. However, in many literatures in power converters, the design of the conventional proportional, integral and derivative (PID) controller based on lead-lag compensators or Z-N method are discussed. The design of different compensators like Lead, Lag and PI controllers using an operational amplifier were discussed for buck-boost converter (Rashid, 2001). The above compensators are designed based on trial and error until the required stability criteria are satisfied.

Viswanathan et al. (2002, 2005) proposed a novel tri-state boost converter to eliminate the RHP zero by incorporating an additional degree of control-freedom. The penalty paid in this method is the inclusion of an additional switch and a diode, which in turn reduces efficiency of the converter. A digital controller design based on root locus technique for buck and boost converters is reported in some papers. The real time implementation of control algorithm using TMS320C50 processor is also presented.

Few literatures in control applications have discussed the controller design based on small signal transfer function model, considering the effect of RHP zero. It has discussed in detail the PID controller design for a system RHP zero. Also it has proposed a method, which improves the transient behaviour of a system with RHP zero when compared to the Z-N method. To improve the robustness against model uncertainties and disturbances, an internal model control (IMC) has been discussed. For DC-DC buck and boost converters, the application of IMC controller is verified by few research work. However the IMC produces robustness at the expense of slower response. An alternative to this method called the Synthesis method can be used to design a simple but robust PID controller for systems with RHP zero. A detailed simulation procedure and results are presented and discussed for DC-DC boost converter with RHP zero by implementing above said methods (Arulselvi, 2007).

However, the linear PID controllers are sensitive to parameter variations, change in operating point, load and supply voltage disturbances. To solve these problems and to provide voltage feed forward control, nonlinear controllers such as a SMC under CMC can be implemented. Many literatures have reported the application of SMC to DC-DC converters. Since DC-DC converters are inherently variable structured, a variable structure type SMC is proposed. Also, a few research papers have reported about the design of SMC under CMC for a DC-DC converter with RHP zero. SMC provides a means to achieve improved transient response and robustness against disturbances. Even though SMC provides stability and robustness, a systematic design procedure of SMC for

the control of converters is not much reported in the literatures (Rashid, 2001). A few papers have reported about the design procedure of a practical sliding mode voltage controller for buck converter and for pole converter (He and Luo, 2006). Passive SMC strategy is proposed based on passive control with energy shaping and damping injection for boost converter. These design approaches use complicated mathematical expressions, and have not provided a generalised design procedure applicable to different topologies of switching converters. Also the effect of the RHP zero is not adequately addressed and most of the sliding mode controllers are realised using active filters and analogue components. This imposes complexity and lack of flexibility when control laws are to be tuned again.

2 Analysis and design of boost converter

The boost converter is capable of providing an output voltage that is greater than input voltage (Ang, 1995; Batarseh, 2004). A boost converter using an ideal switch Q is shown in Figure 1. The operation of the boost converter can also be divided into two modes, depending on the switching actions of the switch Q (referring Figures 2 and 3).

Figure 1 Circuit schematic of a DC-DC boost converter

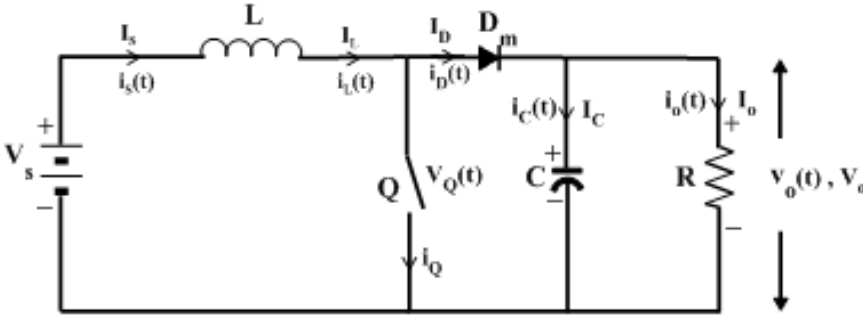

The boost converter consists of a dc supply voltage V_s, boost inductor L, controlled switch Q, freewheeling diode D_m, filter capacitor C and load resistance R. This converter produces an average output voltage (V_o) at a level higher than the supply voltage (V_s). The switch is turned ON and OFF with a switching frequency, f_s (= $1/T_s$) and with a duty cycle, $D = t_{on}/T$, where t_{on} is the ON time of the switch Q and T_s is the switching period.

Mode1 ($0 < t \leq t_{on}$)

Mode 1 begins when the switch Q is switched ON at t = 0 and it terminates at $t = t_{on}$. The equivalent circuit for mode 1 is shown in Figure 2. The diode D_m is reverse biased since the voltage drop across the switch is smaller than the output voltage. The output current during this t_{on} interval is supplied entirely from the output capacitor C, which is chosen large enough to supply the load current during t_{on} with a minimum specified drop in output current.

Figure 2 Equivalent circuit diagram of boost converter ($0 < t \leq t_{on}$) for mode 1

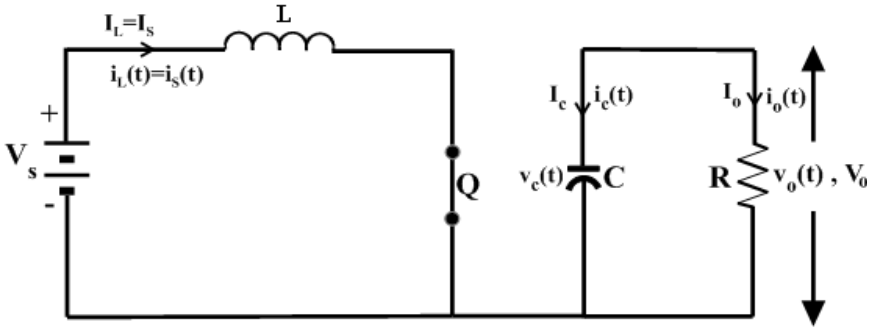

Mode 2 ($t_{on} < t \leq T$)

Mode 2 begins when the switch Q is switched OFF at $t = t_{on}$. The equivalent circuit for this mode is shown in Figure 3. Since the current in the inductor cannot change instantaneously. The voltage in the inductor reverses its polarity in an attempt to maintain a constant current. The current which was flowing through the switch Q will now flow through L, D_m, C and the load R. The inductor current decreases until the switch Q is turned ON again during the next cycle. The inductor delivers its stored energy to the output capacitor C and charges it up via D_m to a higher voltage than the input voltage, V_s. This energy supplies the current and replenishes the charge drained away from the output capacitor when it alone was supplying the load current during the ON time.

Figure 3 Equivalent circuit diagram of boost converter ($t_{on} < t \leq T$) for mode 2

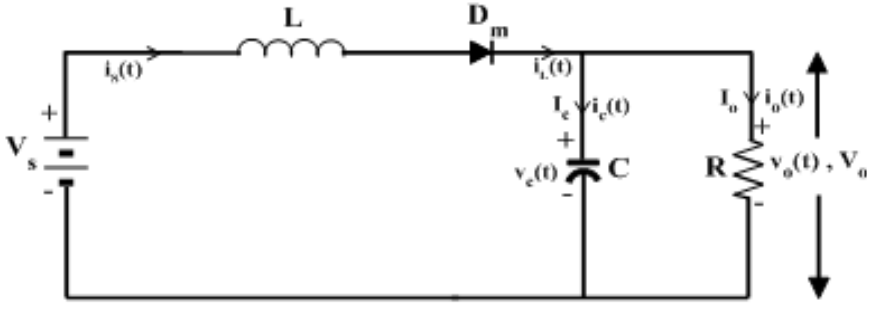

The design parameters considered for DC-DC Boost converter are tabulated in Table 1.

The simulated voltage conversion ratio (M) versus duty ratio (D) for various values of load resistance (R) is shown in Figure 4. The value of M increases steeply for D greater than 0.5. It is seen that, the relation between M and D is nonlinear and M is very sensitive to load variations.

Table 1 Design parameters for DC-DC boost converter

Parameters		*Value*
Supply voltage	V_s	12 ± 2 V
Output voltage	V_o	24V
Inductor	L	43.5 mH
Capacitor	C	220 µF
Resistance of inductance	R_L	0.1 Ω
Electrostatic resistance of capacitance	R_C	0.25 Ω
Load resistance	R	8–16 Ω
Switching frequency	f_S	100 KHz
Load current	I_o	1.5A–3A
DC voltage conversion ratio	M	2

Figure 4 Simulated characteristic curves for M versus D of DC-DC boost converter with different values of R (see online version for colours)

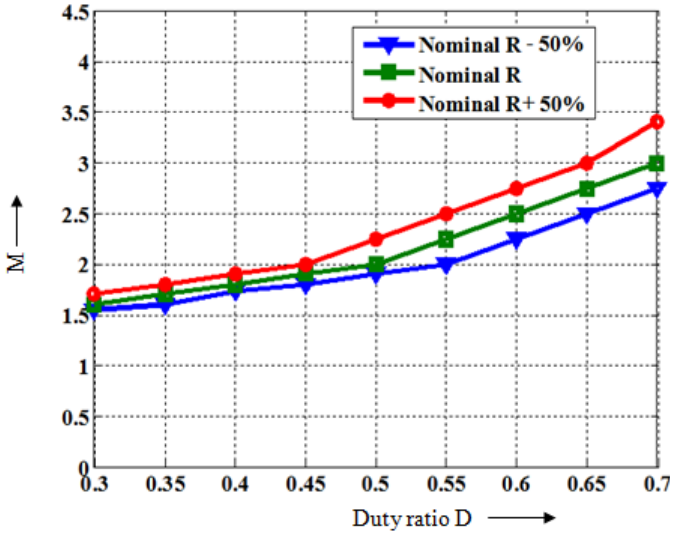

3 Design of conventional proportional plus integral control of DC-DC boost converter with RHP zero

To provide a regulated output voltage for load variations and supply voltage disturbances, it is necessary to have a closed-loop control system. To study the dynamic behaviour of boost converter, its small signal control-to-output transfer function (Arulselvi, 2007) as given as

$$G_{v_o d} = \frac{\hat{v}_o(s)}{\hat{d}(s)} = \frac{K_p(1-\beta s)}{(\tau_1 s+1)(\tau_2 s+1)} \tag{1}$$

The above mentioned transfer function G_{v_od} has a steady state process gain K_p and two poles located at $p_1 = -1/\tau_1$ and $p_2 = -1/\tau_2$. It also has a RHP zero at $z_1 = 1/\beta$ where β is expressed as a function of circuit parameters (Alvarez-Ramirez et al., 2001) as given by

$$\beta = \frac{1}{(1-d)^2 R} \tag{2}$$

Thus in the s-plane, RHP zero moves with the operating point. By substituting the converter parameters as listed in Table 1, equation (1) becomes

$$G_{v_od}(s) = \frac{48 * (1 - 0.017s)}{(0.0147s + 1)(0.002s + 1)} \tag{3}$$

The effect of RHP zero in the open loop converter dynamics can be explained as follows.

Figure 5 Open-loop step response of DC-DC boost converter (see online version for colours)

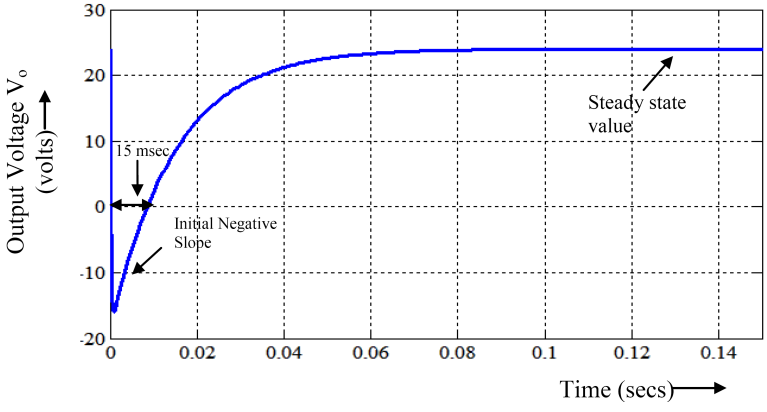

The open-loop response of boost converter for step change in duty ratio (d) from 0.44 to 0.5 assuming initial output voltage of 24 V is shown in Figure 5. It is seen that the response initially takes a negative slope and reaches a negative maximum of –16 V, which is almost 67 percentage of the final positive steady state output value (24 V). Subsequently the response reverses itself and finally reaches a positive steady-state as shown in Figure 5. It takes almost one time constant τ_2 (15 msec) to comeback to zero. Here, the percentage undershoot is directly proportional to the value of β. This particular phenomenon called IR occurs in boost converter due to the presence of inductor, L. For a step increase in d, the output voltage decreases momentarily, since the inductor opposes the initial large change in current (Erickson and Maksimovic, 2004; Viswanathan et al., 2005; Arulselvi, 2007). This effect creates a RHP zero in the control-to-output transfer function restricting the closed-loop bandwidth, thereby limiting the controller gain K_c.

To design linear PI controller, the control-to-output transfer function of the boost converter as given in equation (3) is used. The structure of the PI controller transfer function is given by

$$K_c = 0.00936 \quad \text{and} \quad \tau_I = 2.29 \text{ msec} \tag{4}$$

where K_C is proportional gain, τ_I is the integral time (msec) and K_I is integral gain.

In this work, it is proposed to design a PI controller based on Z-N tuning by frequency response method. By this method the PI controller settings for the boost converter are given as follows

$$K_c = 0.00936 \quad \text{and} \quad \tau_I = 2.29 \text{ msec}$$

The closed-loop simulation of the boost converter is carried out using MATLAB/Simulink software. The converter output voltage is compared with the reference voltage to generate error signal. The PI controller processes the error signal and produces deviation in duty cycle of the switching pulse as the output. The Simulink model of closed-loop control of boost converter is shown in Figure 6.

Figure 6 Simulink model showing closed-loop control of DC-DC boost converter by implementing PI controller

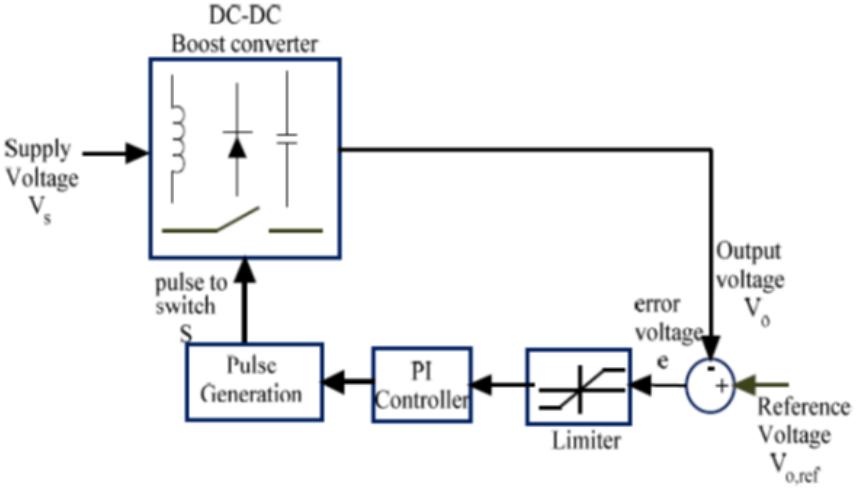

Table 2 Performance indices for simulation results of DC-DC boost converter

	PI controller			*SMC*		
	Settling time T_s(sec)	*Percentage overshoot*	*ISE value*	*Settling time T_s(sec)*	*Percentage overshoot*	*ISE value*
–20% step change in load current	0.8	5	356	0.3	1.45	118
+20% step change in supply voltage disturbances	0.8	8.33	546	0.3	1.25	110

Table 3 Effect of RHP zero on change in reference voltage for DC-DC boost converter

Setpoint change	*PI controller*			*SMC*		
	Settling time T_s(sec)	*Percentage overshoot*	*ISE value*	*Settling time T_s(sec)*	*Percentage overshoot*	*ISE value*
24V to 29V	0.15	4.16	1,456	0.1	1.72	156
29V to 24V	0.13	5.2	1,335	0.06	2.08	154

The results of PI controller are shown in Tables 2 and 3. Since, the design of PI controllers under VMC discussed so far relies on the exact small signal transfer function model of the converter. Hence, the controller performance degrades for wide load current variations and supply voltage disturbances.

To overcome the above shortcomings and to further reduce the effect of RHP zero, CMC can be employed for DC-DC boost converter. Thus CMC can provide voltage feed forward control, overload protection and can eliminate one pole from transfer function making simple feedback design. In the present work, it is proposed to make use of PI controller and SMC with boundary layer for outer voltage loop and inner current loop, respectively. The SMC has the ability to exploit the variable structure nature of DC-DC converters by producing stability even for large supply and load variations. It can also provide robust performance against parameter variations and model uncertainties leading to good dynamic response and simpler implementation.

4 Design of SMC of DC-DC boost converter

The Simulink model of CMC scheme for a DC-DC boost converter is illustrated in Figure 7, where the PI controller and SMC act as outer voltage controller and inner current controller, respectively. The input to the PI controller is the voltage error and the output sets the average reference inductor current for inner current loop. The inputs to the SMC/FSMC are voltage error, e_1 and current error, e_2. The output, u is the control signal, which in turn sets the new duty ratio of the switching pulse to regulate the output voltage V_o.

Figure 7 Simulink model for SMC

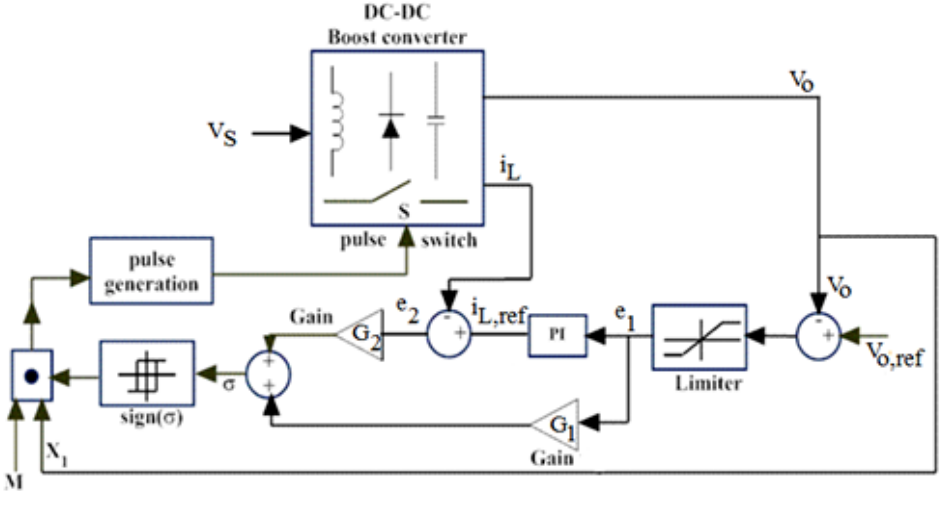

The SMC due to its variable structured nature is more suitable for the control of nonlinear and time varying systems providing robust response under varying operating conditions. The design objective of SMC is to define a sliding surface σ(e, t), to force the plant state vector X, in the presence of model uncertainties and disturbances. Hence it is required to nullify the tracking error vector e=W-X (Davari and Donthi, 1998; Tan, 2005). To

illustrate the effectiveness of the SMC, transfer function of boost converter with RHP zero as given in equation (3) is considered (Alvarez-Ramirez et al., 2001). The vectors X, W and e for boost converter are defined as:

$$W = \begin{bmatrix} w_1 & w_2 \end{bmatrix}^T, \quad X = \begin{bmatrix} x_1 & x_2 \end{bmatrix}^T \quad \text{and} \quad e = \begin{bmatrix} e_1 & e_2 \end{bmatrix}^T \tag{5}$$

where the state variables are considered as $x_1 = v_c = V_o$, $x_2 = i_L$, $w_1 = V_{o,ref}$ and $w_2 = I_{L,ref}$. The values of errors e_1 and e_2 are given by

$$e_1 = w_1 - x_1 = V_{o,ref} - V_o \tag{6}$$

$$e_2 = w_2 - x_2 = I_{L,ref} - I_L \tag{7}$$

To derive the sliding surface σ(e, t), the phase variable canonical form representation of the system is considered. The state space model of the boost converter is given by

$$\dot{\mathbf{X}} = \mathbf{AX} + \mathbf{Bu}; \quad \mathbf{y} = \mathbf{CX} \tag{8}$$

where $A = \begin{bmatrix} 0 & 1 \\ -26{,}123 & -454.5 \end{bmatrix}$, $B = \begin{bmatrix} 0 \\ 1 \end{bmatrix}$ and $C = [569.9e3 \quad -867.9e3]$.

The Filippov's average equivalent switch control u_{eq} (Slotine and Sastry, 1983; Mattavelli et al., 1997; He and Luo, 2006; Arulselvi, 2007) that guarantees $\dot{\sigma}(e, t) = 0$, is obtained as

$$\dot{\sigma}(e, t) = G\dot{e} = G\left(\dot{W} - AW + Ae - Bu_{eq}\right) = 0 \tag{9}$$

$$u_{eq} = (GB)^{-1}G\left[\dot{W} - AW + Ae\right] \tag{10}$$

The error dynamics is given as

$$\dot{e} = \left[1 - B(GB)^{-1}G\right]Ae = A_{eq}e \tag{11}$$

If $(GB)^{-1}$ exists, the vector G is derived by selecting the eigen values of A_{eq} such that it guarantees the asymptotic convergence of error to zero at the desired rate. The matrix A_{eq} is chosen to satisfy (11) and is given by

$$A_{eq} = \begin{bmatrix} -1 & 0 \\ 0 & -1 \end{bmatrix}$$

The matrix G is then obtained using equation (11) as

$$G = \begin{bmatrix} G_1 & G_2 \end{bmatrix} = [0.002 \quad 1]$$

Hence, the sliding surface σ is

$$\sigma = G_1e_1 + G_2e_2 \tag{12}$$

Equation (12) shows that, if the boost converter operates in sliding mode ($\sigma = 0$), the dynamics of errors e_1 and e_2 tend exponentially to zero with a time constant G_2/G_1. Since during step transients, the converter is in the reaching mode, the time constant G_2/G_1 cannot be designed to originate error variations larger than allowed by a maximum permissible value of current i_L (Rashid, 2001). Hence for this application G_1 and G_2 are

found to be 0.002 and 1, respectively. Also the error state equation given in equation (11) describes the error motion under SMC. Once the sliding surface σ (e, t) = Ge is derived then the control law is defined as

$$u = M\ \mathrm{sgn}(\sigma)x_1 = Ux_1 \tag{13}$$

where $U = \begin{cases} 1, & \text{for } \sigma > \delta \\ \text{Previous U}, & \text{for } -\delta \le \sigma > \delta \\ 0, & \text{for } \sigma < -\delta \end{cases}$ and δ is positive constant.

To achieve minimum chattering, δ is chosen as 0.01. This value is selected by iterative procedure. The equation (13) is used to generate the duty ratio of gating pulse to MOSFET, which in turn regulates the output voltage deviation. Here M is a constant unity gain chosen so that the reaching condition, $\sigma\dot{\sigma} < o$ is satisfied. The reaching condition ensures that the tracking error trajectory is asymptotically attracted to σ = 0. It is observed that the control law u as given in equation (13) does not depend on system operating conditions, plant parameters or bounded disturbances. This is achieved as long as the control input u is large enough to maintain the plant subsystem in sliding mode. Therefore, it is said that the plant dynamics, operating in sliding mode, is robust against the disturbances as mentioned. The desired dynamics of the output variable y is determined only by the coefficient G of control law. The generation of control signal for SMC is shown in Figure 8. Due to discontinuous nature of control signal u, chattering is produced.

Figure 8 Generation of control signal for SMC

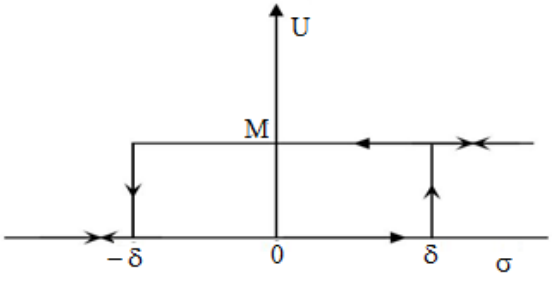

The voltage error e_1 and current error e_2 are calculated and sum of the gain product of errors producing the sliding function, σ. Based on the magnitude and sign of σ, the control signal produces the gating pulse to switch S, which in turn regulates the output voltage. The sliding function is found to be chattering within the boundary of ±0.01 and hence it never reaches the sliding surface.

Using Z-N technique, the outer PI controller parameters K_c and K_I are obtained from process reaction curve drawn for boost converter with SMC control in the inner loop. A step change in $i_{L,ref}$ is applied to the inner current control with outer voltage loop in open condition. Then the output voltage is traced as process reaction curve. The curve is obtained by giving a ±36% step change in reference inductor current from nominal value. The values of proportional gain K_c and K_I are calculated as 0.82 and 0.99 respectively.

Figure 9 Regulated output voltage for sudden change in reference voltage from 24 V to 29 V applied at 0.5 sec and 29 V to 24 V applied at 0.8 sec by implementing SMC (see online version for colours)

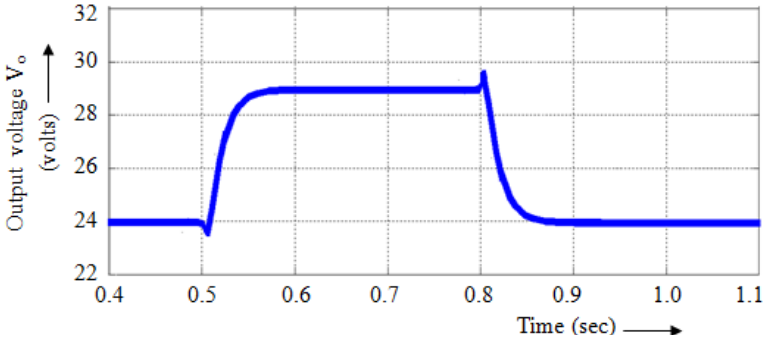

Figure 10 Waveforms of switching pulse and sliding function (σ) for sudden reference voltage change from 24 V to 29 V by implementing SMC (see online version for colours)

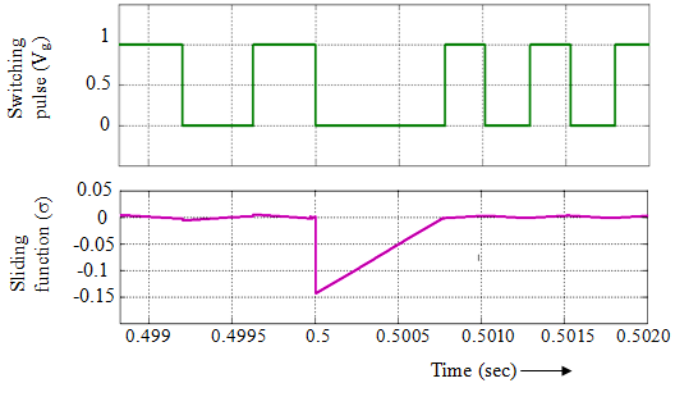

Figure 11 Waveforms of switching pulse and sliding function (σ) for sudden reference voltage change from 29 V to 24 V by implementing SMC (see online version for colours)

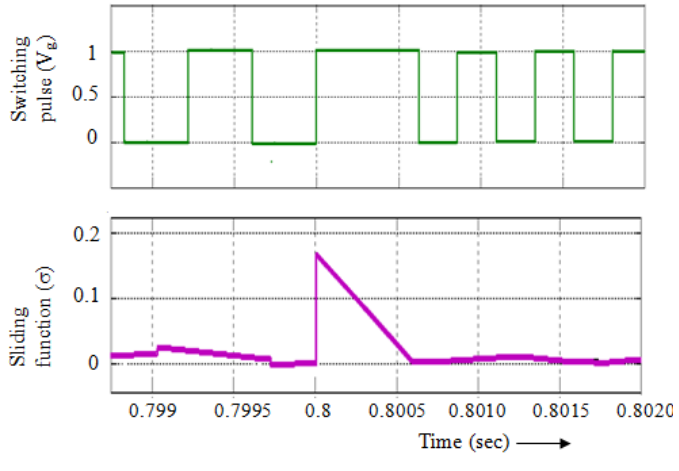

Figure 12 Waveforms of regulated output voltage, switching pulse and sliding function (σ) for 20% step decrease in load current by implementing SMC (see online version for colours)

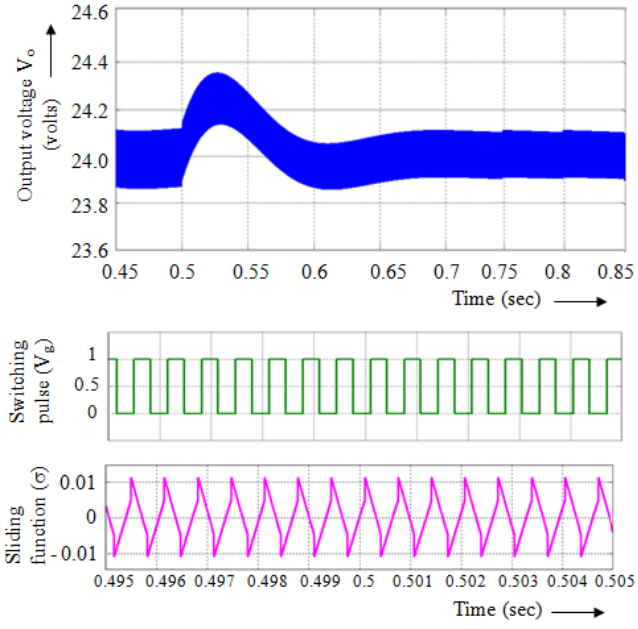

Figure 13 Waveforms of regulated output voltage, switching pulse and sliding function (σ) for 20% step increase in supply voltage by implementing SMC (see online version for colours)

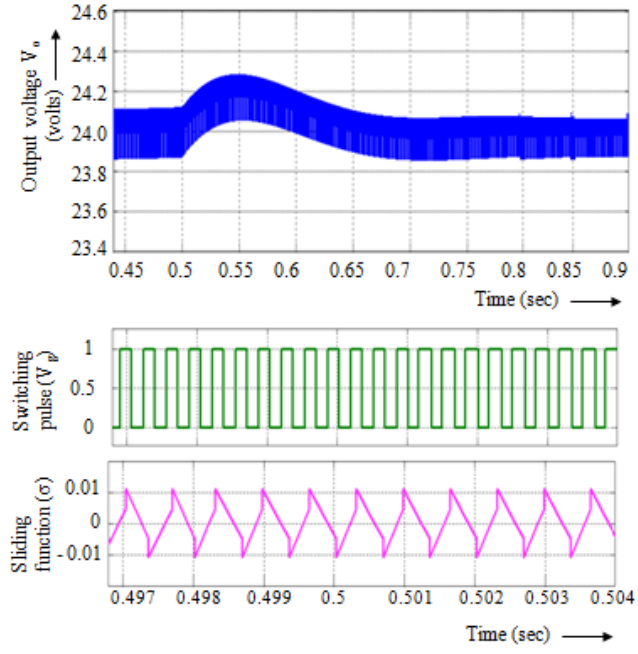

The regulated output voltage for reference voltage change of 24 V to 29 V applied at 0.5 sec and 29 V to 24 V applied at 0.8 sec is shown in Figure 9. It is seen that percentage initial drop due to RHP zero is reduced to 1.72% which is less than PI controller response. Also it is observed that, when sliding function σ is within the boundary layer ±0.01, previous duty ratio is maintained. When σ exceeds the boundaries ±0.01, the switch is either fully ON or fully OFF as shown in Figures 10 and 11.

The dynamic performance is also studied for a step change in load current variations of –20% is made at t = 0.5sec and +20% step change in supply voltage disturbance is made at t = 0.5sec. The simulation results of regulated output voltage, switching pulse and sliding function for load variation and supply voltage disturbance are presented in Figure 12. The sliding function is chattering within the boundary layer and it is not changed due to the above disturbances. The results reveal that the controller is immune to supply disturbances and load variations.

Figure 12 shows that the output voltage settles well within 0.3 sec and with a percentage overshoot of 1.45. Similarly Figure 13 shows that the output voltage settles after a supply disturbance within 0.3 sec and with a percentage overshoot of 1.25. The sliding function is chattering within the boundary of ±0.01 and hence it never reaches the sliding surface. The results obtained from closed-loop simulation using conventional PI and sliding mode controller for DC-DC boost converter are tabulated in Tables 2 and 3.

5 Conclusions

Non-minimum phase plants cause fundamental design constraints, such as bandwidth limitation, in the feed-back control systems due to their peculiar phase characteristics. Therefore, the control problem of non-minimum phase systems is quantifiably harder than the minimum phase's one. Furthermore, the control problem becomes more severe in the presence of system uncertainties and external disturbances. This work proposes linear controller (PI) and nonlinear controller (SMC) for closed-loop voltage regulation of DC-DC boost converter with RHP zero. The derivation of the controller algorithms are presented and verified by simulations using MATLAB/Simulink software. It is observed that SMC is robust to supply disturbances and load current variations. It produces zero steady state error with reduced undershoot due to non-minimum phase characteristic. However, it produces chattering in control signal. The performance measures for PI and SMC in simulation are calculated and compared. It is concluded that SMC is a better choice for voltage regulation of DC-DC boost converter. The proposed control methods can be used for low power switch mode power supply applications and can be extended for high power applications also.

References

Alvarez-Ramirez, J., Cervante, L., Espinosa-perez, G., Maya, P. and Morales, A. (2001) 'A stable design of PI control for DC-DC converters with an RHS zero', *IEEE Trans. on Circuit and Systems-I: Fundamental Theory and Applications*, Vol. 48, No. l, pp.103–106.

Ang, S.S. (1995) *Power Switching Converters*, Marcel Dekker, Inc, New York.

Arulselvi, S. (2007) *Conventional and Intelligent Control of Hard Switched and Soft Switched DC-DC Converters*, PhD dissertation, Anna University, Chennai.

Batarseh, I. (2004) *Power Electronic Circuits*, John Wiley and Sons, Inc., India

Davari, A. and Donthi, A. (1998) 'Stable robust tracking of non-minimum phase systems', *Proc. IEEE International Conf.*, pp.380–387.

Erickson, R.W. and Maksimovic, D. (2004) *Fundamentals of Power Electronics*, Kluwer Academic Publishers, Norwell.

He, Y. and Luo, F.L. (2006) 'Sliding-mode control for DC-DC converters with constant switching frequency', *IEE. Proc. Control Theory Appl*., Vol. 153, No. l, pp.37–45.

Mattavelli P., Rossetto L. and Spiazzi G. (1997) 'Small-signal analysis of DC-DC converters with sliding mode control', *IEEE Trans. on Power Electronics*, Vol. 20, No. 2, pp.425–437.

Rashid, M.H. (2001) *Power Electronics Hand Book*, Academic Press, New York.

Slotine, J.J. and Sastry, S.S. (1983) 'Tracking control of non-linear systems using sliding surface, with applications to robot manipulators', *Int. J. Control*, Vol. 38, No. 2, pp.465–492.

Tan, S-C., Lai, Y.M., Cheung, M.K.H. and Chi, K.T. (2005) 'On the practical design of a sliding mode voltage controlled buck converter', *IEEE Trans. on Power Electronics*, Vol. 20, No. 2, pp.425–437.

Viswanathan, K., Oruganti, P. and Srinivasan, D. (2005) 'Dual-mode control of tri-state boost converter for improved performance', *IEEE Transactions on power electronics*, Vol.20, No. 4, pp.790–797.

Viswanathan, K., Srinivasan, D. and Oruganti, R. (2002), 'A universal fuzzy controller for a non-linear power electronic converter', *Proc. IEEE International Conf.*, pp.46–51.